Journal of Structural Geology 29 (2007) 924–932

JOURNAL OF STRUCTURAL GEOLOGY

www.elsevier.com/locate/jsg

Tectonic thickening of hanging-wall units over a ramp

Hemin A. Koyi [a,*], Bertrand Maillot [b]

[a] Hans Ramberg Tectonic Laboratory, Department of Earth Sciences, Uppsala University, Villavägen 16, 752 36 Uppsala, Sweden
[b] Departement des Sciences de la Terre et de l'Environnement, Université de Cergy-Pontoise, Laboratoire de Tectonique, UPMC, UCP, CNRS, 5 mail Gay Lussac, Neuville-sur-Oise, 95031 Cergy-Pontoise Cedex, France

Received 30 September 2006; received in revised form 19 February 2007; accepted 21 February 2007
Available online 12 March 2007

Abstract

In this article, we use results of analogue models and published numerical models to study the elements that influence the amount of thickening of hanging-wall units during their transport over a ramp. The models, consisting of granular layers, were shortened over a single-pass, rigid ramp dipping at 15, 30 or 45° and friction coefficient (μ) that was large (0.67), intermediate (0.42) or null. Model results show that the amount of thickening depends on the ramp angle and its friction. Thickening increases dramatically with increasing ramp friction and dip. The maximum amount of thickening (80%) is observed over steepest ramps (45°) with largest ramp friction ($\mu = 0.67$), whereas the minimum amount of thickening (2.5%) occurs over frictionless ramps dipping 15°. For the same friction coefficient along the ramp, steeper ramps cause larger amounts of thickening. The tectonic thickening demonstrated by our models was compared with thickening of hanging-wall units of natural examples, and other experimental and model studies. This comparison shows that thickening occurs whether the material considered is brittle, viscous, or plastic. It also confirms the importance to thickening of ramp angle and fault friction. Finally, it reveals also that ramp shape (round or sharp bend), its changes due to footwall deformations, and the topographic relief, are additional boundary conditions for thickening. More generally, our model results and other published model results demonstrate that retardation during the transport of hanging-wall units over a ramp results in hanging-wall thickening.
© 2007 Elsevier Ltd. All rights reserved.

Keywords: Kinematic models; Hanging wall; Thickening; Modeling; Ramp friction; Ramp dip

1. Background to the problem

Kinematic models, which do not incorporate force or rheology, create area-balanced sections by prescribing geometric relationships. The "fault-bend fold" is an early example (Rich, 1934; Willis and Willis, 1934; Dahlstrom, 1969), which refers to layered rocks that fold in response to translation over a ramp. More detailed geometric and kinematic models were developed later for fault-bend folds (Suppe, 1983; Jamison, 1987; Mitra, 1992), fault-propagation folds (Suppe, 1985; Jamison, 1987; Chester and Chester, 1990; Mitra, 1990; Suppe and Medwedeff, 1990; McNaught and Mitra, 1993; Mercier et al., 1997), fault-displacement-gradient folds (Wickham, 1995), detachment folds (Jamison, 1987; Mitra, 1992; Poblet and McClay, 1996), and break-thrusts (Fischer et al., 1992).

Kinematic models are beneficial for the geometric interpretation of faulted and folded terranes and a variety of geometric rules can be applied to constrain the kinematics of fault-cored folds (for details see Suppe, 1983; Dahlstrom, 1990; Withjack and Peterson, 1993). Ramsay (1992), however, addressed some geometric problems of ramp-flat thrust models and emphasized the need for modification of the models to fit the geological data. Likewise, Kattenhorn (1994) argued for developing new models since kinematic models fail to account for features identified in outcrop-scale structures. He argued that the assumption of conservation of layer-thickness breaks down for ramp angles exceeding 30°, and at progressively smaller angles in the case of imbricate stacks.

* Corresponding author. Tel.: +46 18 471 2563; fax: +46 18 471 2591.
E-mail address: hemin.koyi@geo.uu.se (H.A. Koyi).

0191-8141/$ - see front matter © 2007 Elsevier Ltd. All rights reserved.
doi:10.1016/j.jsg.2007.02.014

Our present contribution is motivated by the fact that all models of fault-bend, and fault-propagation folds (except Cristallini and Allmendinger, 2002) assume conservation of bed thickness at the lower flat-ramp transition. In an earlier article (Maillot and Koyi, 2006), we used a theoretical approach (Maillot and Leroy, 2003), backed by results of sand models, to quantify the refraction of back-thrust dips in hanging-wall units as they were transported above a ramp. Maillot and Koyi's results (Maillot and Koyi, 2006) were not in agreement with predictions from kinematic models where the dip of back-thrusts is unrealistically steep. In this contribution, we use the results of sand models to quantify the effect of ramp dip and friction on the thickness change of hanging-wall units transported above a single-pass rigid footwall ramp. We also use natural examples and results of previously published models to argue for hanging-wall thickening not considered in some commonly used kinematic models. The thickening of hanging-wall units during their transport over a ramp is referred to as ''tectonic thickening'' throughout this article. We focus only on the deformation of the hanging-wall layers and do not include deformation of the footwall in our modeling.

2. Description of sand models

The measurement of friction and mechanical properties of the granular materials, the details of the experimental procedures, and the experiments at 30° and 45° are all described in Maillot and Koyi (2006). Here, we have added three experiments for 15° ramp to complete the study of the thickening effect. For coherence, we kept the two-layer structure that was originally designed to study thrust refraction. In total, a series of nine experiments were made with a simple set-up (Figs. 1 and 2). A model made of two layers of Nemours sand separated by a thin layer of micro glass beads, with respective thicknesses of 10, 1, and 9 mm, was placed in a 200 × 200 × 100 mm Plexiglas box in which a rigid Plexiglas ramp was installed before hand. To shorten the models, a rigid ramp, simulating footwall units, was pushed into the granular layers at a constant velocity. Any topography that formed during shortening was eroded at every 10 mm of shortening. Thus the boundary conditions remained constant throughout the experiment, and the passage of sand into the hanging wall quickly reached a steady-state behavior. In all experiments we have tried to be consistent during the preparation of the layers; pouring sand in small amounts on the surface of the model and scraping the sand pile to a horizontal layer, not more than 3 mm thick at a time. Colored marker

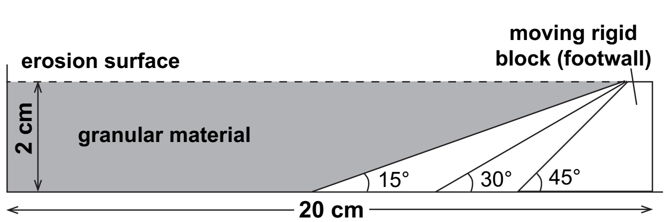

Fig. 1. Line drawing of the 2-dimensional model setup.

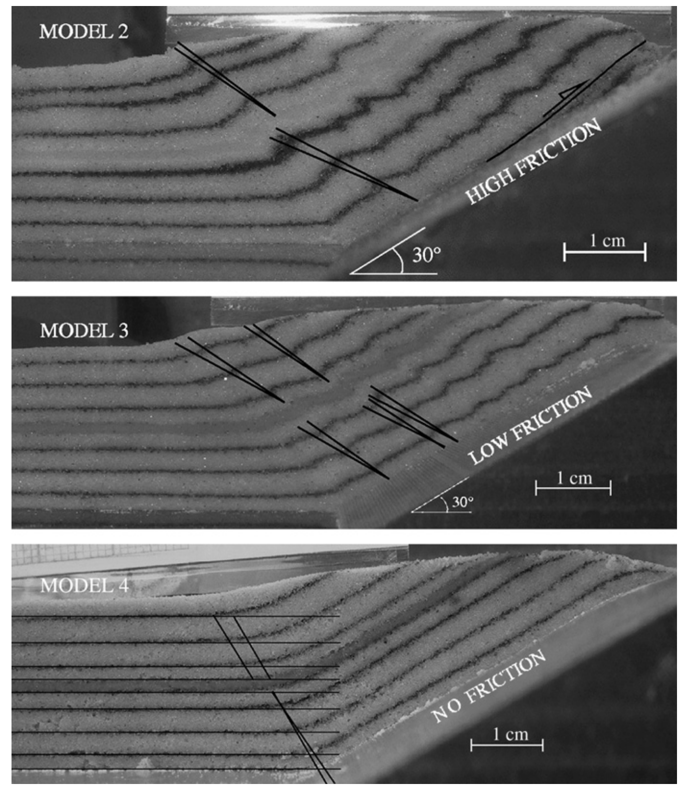

Fig. 2. Sections of models with 30° ramp at final stage of deformation (from Maillot and Koyi, 2006).

horizons (each about 0.1–0.3 mm thick) were sprinkled on the surface after each scraping step, to act as strain markers. This somewhat laborious procedure has the central advantage of providing reasonably reproducible samples. The models, which were 20 mm thick, were shortened in a 200 × 200 mm box. Boundary effect was visible within a 1.5–2 cm wide zone along the boundary of the box. However, our measurements were made along cross sections, which were cut in the middle of the models away from the boundary effect. These models are a follow-up of a previous study where similar models were used to validate the mean dissipation theory and verify the mechanism for thrust refraction (Maillot and Koyi, 2006).

In experiments with large friction, a P150 sandpaper (particles of 97 μm in average) was glued on the ramp, providing a larger friction ($\mu = 0.67$) than the internal sand friction (0.61). In experiments with intermediate friction ($\mu = 0.45$), a fiberglass sheet was glued on the ramp. In experiment with no friction, the ramp was slid under a fiberglass sheet above which the model was placed, thus providing a zero friction surface since there was no relative displacement between the sand and the fiberglass sheet during the transport of the sand layers over the ramp. Alternatively, the ramp can be lubricated as in Merle and Abidi (1995), allowing for base parallel contraction of the hanging wall, but at the cost of making a rounded ramp. Both methods yield very low thickening figures.

Every model was then shortened by pushing the rigid ramp into the model at a constant velocity of 22 cm/h. We chose to push the ramp into the sand layer rather than the sand layer towards the ramp because in the latter case, the sand would deform at the contact with the piston instead of along the imposed ramp. The consequences of this choice on thickening will be discussed in the final section. The total applied shortening was in all cases sufficient to reach a steady state in the model. Once the maximum shortening allowed by the geometry of the box was reached, the model was wetted and sections cut parallel to the shortening direction (i.e. perpendicular to the ramp), were photographed.

The Nemours sand used in the models was provided by the Division Géologie, Géochimie of the Institut Francais du Pétrole. It is a natural sand sieved between 80 and 120 μm with a sharp peak at 100 μm. Its density is 1.53 ± 0.02 g/cm^3 as measured by slowly pouring the sand in the container. The internal friction of the Nemours sand was computed from a linear regression of the measured data with error bars. The friction angle is 30.3–32.9 and the cohesion is 80 ± 22 Pa. The friction of the Nemours sand against the P150 sandpaper and the fiberglass sheet was determined by similar measurements for the internal friction of the sand. The results and the linear regression show that friction angle is 34.5–34.9 for the sandpaper and 22.8–23.4 for the fiberglass sheet, with respective cohesions of -20 ± 6 Pa and 51 ± 11 Pa.

In choosing the ramp parameters, we have tried to cover the realistic values of dip and friction, and at the same time provide a systematic approach by choosing other values, which may differ from what has been suggested for natural values. In the first three experiments, the ramp dip was 15°, in the second three experiments, it was 30° and in the third group it was 45°. For each ramp dip, friction varied from large (static friction coefficient = 0.67), intermediate (static friction coefficient = 0.45) to null (static friction coefficient = 0). Although the large and the intermediate friction coefficient values may be large compared to in natural cases, these values were chosen merely to illustrate the systematic effect of friction on hanging-wall thickening. Smaller values would have not given as clear a difference as these larger values do. These values, which are the coefficients of static friction, are likely to be less than the coefficient of sliding friction; i.e. during the transport of the sand layers along the ramp. In addition, in laboratory experiments, large coefficients of friction along rock surfaces are documented (Marone et al., 1999; Di Toro et al., 2004). Di Toro et al. (2004) used an apparatus that applied rotary shear at ambient temperature and humidity to rock samples (Novaculite; a meta sedimentary rock composed mostly of microcrystalline quartz and is a recrystallized variety of chert) to study the strength of frictional contact between rock surfaces. They found that the coefficient of friction, which was 0.6–0.7 at low sliding velocities (up to 1 mm/s), decreased dramatically to values as small as 0.2 at larger shearing velocity (>1 to 10 mm/s). They also showed that this effect was transient; the coefficient of friction returns to large values on returning to lower shear velocity. Laboratory data also show that mineralogy of the gouge materials influence the coefficient of friction along the fault surface. Marone et al. (1999) conducted laboratory tests to study the role of clays in determining the mode of slip (seismic versus aseismic) within subduction zone megathrusts. They reported that, in contrast to what was widely expected, illite shale exhibited velocity-strengthening behavior and possessed a coefficient of friction ranging from 0.42 to 0.68 over a range of normal stresses from 5 to 150 MPa and sliding velocities from 0.1 to 200 μm/s. In contrast, smectite sheared under identical conditions exhibits small friction ($\mu = 0.15{-}0.32$) and a transition from velocity weakening at low normal stress to velocity strengthening at higher normal stress (>40 MPa).

3. Hanging-wall deformation

Several modeling studies have shown that during their transport over a ramp, hanging-wall units deform (Wiltschko, 1979; Berger and Johnson, 1980; Kilsdonk and Fletcher, 1989; Erickson and Jamison, 1995; Strayer and Hudleston, 1997). Berger and Johnson (1980) and Kilsdonk and Fletcher (1989) were amongst the first who used analytical approaches to study the mechanics of folding in viscous hanging-walls over a rigid or deformable footwall ramp, respectively. Apperson and Goff (1991) used a finite-element modeling approach to conclude that foreland-ward ramp translation and accompanying deformation depend on the mechanical properties of the deformed units and ramp dip. Chester et al. (1991) demonstrated hanging-wall deformation in experiments with layers of sandstone and mica or lead deformed in a triaxial rig. Later numerical models used viscous-plastic (Erickson and Jamison, 1995), elastic-plastic (Strayer and Hudleston, 1997), and elastic-plastic and cohesion-softening materials (Erickson et al., 2001) to investigate the deformation associated with hanging-wall transport over a ramp. Koyi (1995), Koyi and Vendeville (2004) and Koyi et al. (2004) quantified tectonic compaction in sand models to argue that tectonic thickening accommodated part of the shortening as layers in front of a wedge were incorporated into new thrust imbricates. The cases show that tectonic thickening may occur in brittle materials by faulting and in ductile materials by continuous flow. Therefore the rheological nature of the material does not favor or inhibit thickening.

4. Tectonic thickening

Three ramp dips were chosen in this study; 15°, 30° and 45°, and we did not see the need to do the same analysis for ramp dips lower than 15° or higher than 45°. Below 15°, the hanging-wall deformation becomes difficult to identify. Above 45° on the other hand, an imposed ramp is usually shortcut by a less steep spontaneous ramp in the loose sand (Maillot et al., 2007), unless the ramp possesses a very small friction or the topographic build up is eroded as soon as it forms. Hence, the systematic study of thickening effect cannot be applied to very steep ramps.

We define the thickening as (eo – ei)/ei, where the undeformed thickness ei of the layers above the flat is measured directly from the cross sections, and the deformed thickness, eo, of the hanging wall is also measured directly from the cross sections. Results of our models show not only that the hanging-wall units thicken, but also that the amount of thickening depends on both the dip of the ramp and friction along the ramp (Fig. 3). The models show that least thickening (2.5% of initial thickness) takes place where friction along the gently dipping ramp (15°) is zero (Fig. 3A). The effect of ramp dip on deformation is obvious in the model with frictionless steep ramp (45°), where the hanging-wall units were thickened by 15% (Fig. 3B). However, the maximum amount of thickening (80% of the initial thickness) is observed over a high-friction ramp that dips 45° (Fig. 3B). This can be contrasted with the case (high ramp friction, but gentle ramp dip = 15°), where the hanging-wall units were thickened only by 20% (Fig. 3B).

Several studies have focused on the effect of friction along the decollement on the evolution of a thrust belt (Davis and Engelder, 1985; Letouzey et al., 1995; Cotton and Koyi, 2000; Smart and Couzens-Schultz, 2001; Bahroudi and Koyi, 2003; Koyi and Cotton, 2004). However, in this study we focus only on the influence of ramp friction on the deformation of the hanging-wall units. The effect of ramp friction is demonstrated by models that had similar ramp dip, but different ramp friction (Fig. 3A). A frictionless ramp (dipping 15°) caused 2.5% thickening, whereas a high-friction ramp with the same dip (15°) caused almost one magnitude larger (20%) thickening. The effect of ramp friction is enhanced in steeper ramps (Fig. 3A,B). Model measurements show that hanging-wall thickening is governed by both the friction along and the dip of the ramp, which they are transported over (Fig. 3). The effect of relief build-up is illustrated in Fig. 3C and will be commented on in the next section.

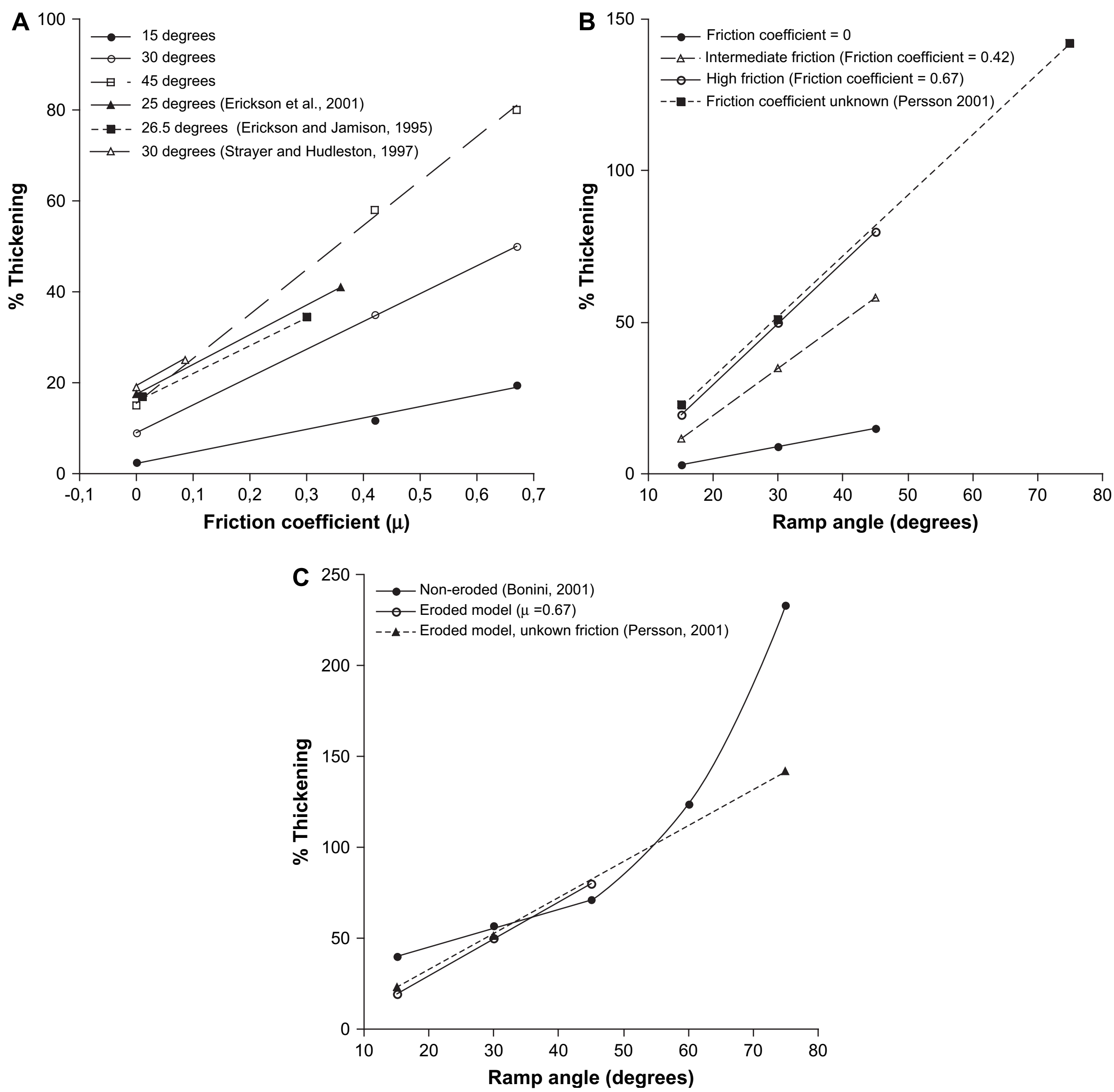

Fig. 3. Plots showing the effect of ramp friction (A) and ramp dip (B) on thickening of hanging-wall units transported over a ramp. (C) Comparison of hanging-wall thickening versus ramp angle in eroded and non-eroded models. The amount of thickening is calculated relative to the initial thickness of the undeformed layers. Unless specified, the data come from our own models.

In our own models, we have not studied the effect of internal friction of the deformed layers on the amount of thickening. However, judging from results of earlier models (e.g. Koyi et al., 2004), where granular layers with smaller coefficient of internal friction underwent less compaction, we assume that tectonic thickening increases with increasing the coefficient of internal friction of the deformed layers. The dissipation theory of Maillot and Leroy (2003, Fig. 3B) also predicts the same trend, equivalent in magnitude to the effect of ramp dip, and less than the effect of ramp friction.

5. Natural and experimental examples

To support the interpretation of our model results, below we present thickening measurements from several natural, experimental and numerical examples. For the first natural example, we measured thickening of carbonate layers that are shortened above a ramp in the Rockies (Fig. 4A). The layers are deformed above an out-of-sequence ramp (dips 35°) that lies in a steep limb of a fold. Thickness was measured in two ways; one perpendicular to the ramp and the other perpendicular to the bedding. Both measurements show 15% to 12% thickening, respectively. Since the mechanical properties at the time of deformation are not known, it is difficult to estimate the friction coefficient along the ramp.

In our second natural example, we measured hanging-wall thickening above a salt detachment from a seismic line published by Cook and MacLean (1999) (Fig. 4B). Our measurements give a very low value of thickening (4.5% to 8%), which could be attributed to either hanging-wall units above the flat are already thickened by an out-of-sequence thrust and/or small friction along the ramp due to the presence of a salt detachment. In this example, both the ramp dip and friction change; the ramp steepens upward; and its friction is likely to increase as it cuts from the salt layer into clastic units upwards. In this example, the measured thicknesses are in time rather in distance. However, we assume that the depth-converted version of this example would not result in much difference in the thickening since there are no major lateral changes in lithology or their dips.

In the third example (Fig. 4C), which is from Stellarton (Nova Scotia), both the footwall and hanging-wall units were deformed. In this example, a siderite band embedded within a layer of shale (Pennsylvanian Stellarton Formation) shows thrust duplication where both footwall and hanging-wall have undergone 9% and 11% thickening, respectively (Fig. 4C) above a ramp which dips ca. 18°. This example illustrates that even when the footwall is involved in the deformation, the units above the ramp show considerable thickening.

These three natural examples show the existence of a thickened hanging wall above a ramp. Magnitude of ramp friction and other material properties are not known, but they do show the existence of the modeled phenomenon.

Turning to experimental and numerical studies where material properties are known, we used Chester et al.'s models (Chester et al., 1991), which were deformed in a triaxial rock-deformation apparatus at room temperature and at 50-MPa

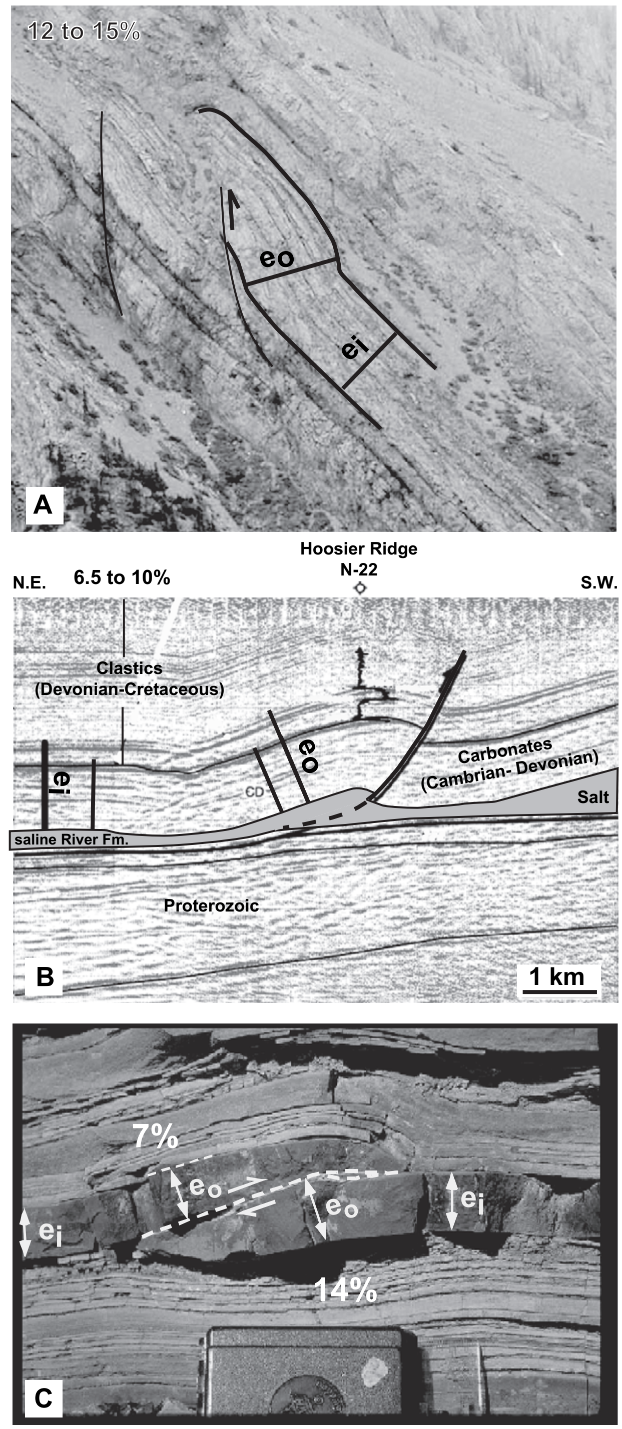

Fig. 4. Natural examples used to estimate tectonic thickening from. The black bars indicate the measured thicknesses perpendicular to the ramp. (A) Out-of-sequence faulting in the Canadian Rocky Mountain (photo by Dengfa He; http://geoweb.princeton.edu/research/SSG/images/outsequence.jpg). The ramped sequence is thickened by 12% (measured perpendicular to bedding) to 15% (measured perpendicular to the ramp). (B) Interpreted seismic line across the Hoosier ridge, showing detachment in the Saline River Formation (slightly modified from Cook and MacLean, 1999) s, Upper Cambrian Saline River Formation; D, Cambrian to Devonian carbonates, undivided. (C) Thrust duplication of a single bed; example of a fault-bend fold with deformation in both footwall and hanging wall (Pennsylvanian Stellarton Formation shales and siderite band, Stellarton, Nova Scotia; Waldron, 2004).

confining pressure. The models consisted of a single layer of sandstone containing a saw-cut ramp that is inclined 20° to the layering, and an overlying, intact, thinly layered unit that is composed of limestone inter-layered with lead or mica. Similar to our sand models and the natural examples, the layered pack in Chester et al.'s experiments, which were unscaled, thickened during its transport over the ramp by 18–27% above the ramp area (Chester et al., 1991, Fig. 5A).

Considering other sandbox experiments (Bonini, 2001; Persson, 2001), tectonic thickening was also observed. For an eroded model similar to our experiments (Persson, 2001), tectonic thickening of ca. 32% remained constant regardless of the amount of bulk shortening. However, for non-eroded models, tectonic thickening increased with bulk shortening and ramp angle (Bonini, 2001; Persson, 2001), which is consistent with overcoming a larger vertical load to translate the hanging wall rocks forward.

The tectonic thickening observed in sand models is also observed in numerical model results. Strayer and Hudleston (1997) used the finite-difference program FLAC (Fast Lagrangian Analysis of Continua) to study the initiation of folding and plastic deformation associated with a ramp (dipping 30°) in a pre-existing thrust fault (Fig. 5B). Measurements of the hanging-wall units in their models shows that, in addition to thickening of the hanging-wall units over a frictionless ramp, increasing ramp friction results in an increase of the amount of hanging-wall thickening (Fig. 3A). Similarly, thickening measurements in Erickson and Jamison's numerical models (Erickson and Jamison, 1995) show that hanging-wall units thicken twice as much (34%) over a frictional ramp ($\mu = 0.3$) compared to (17%) over a frictionless ramp ($\mu = 0.01$) (Fig. 3A). In both cases, the ramp dip was 26.5°. Thickening was also observed for all simulated rheologies: viscous (7.5%), viscoelastic (12%), and plastic (27.5%) with the additional effect that thickening was greater when the footwall behaved rigidly.

Erickson et al. (2001), who used the same numerical code (FLAC) as Strayer and Hudleston (1997), investigated the effects of fault geometry, fault friction, material properties and anisotropy on whether hanging-wall units deform by bedding parallel slip or back-thrusting during their transport above a ramp. In their models, the ramp friction was $\mu = 0.36$ (Fig. 5C), or $\mu = 0$ (Fig. 5D). In each case, the bend (hinge) separating the basal flat from the ramp was either sharp or rounded. Measuring thicknesses in the hanging wall units of these simulations, shows that thickening over a frictionless

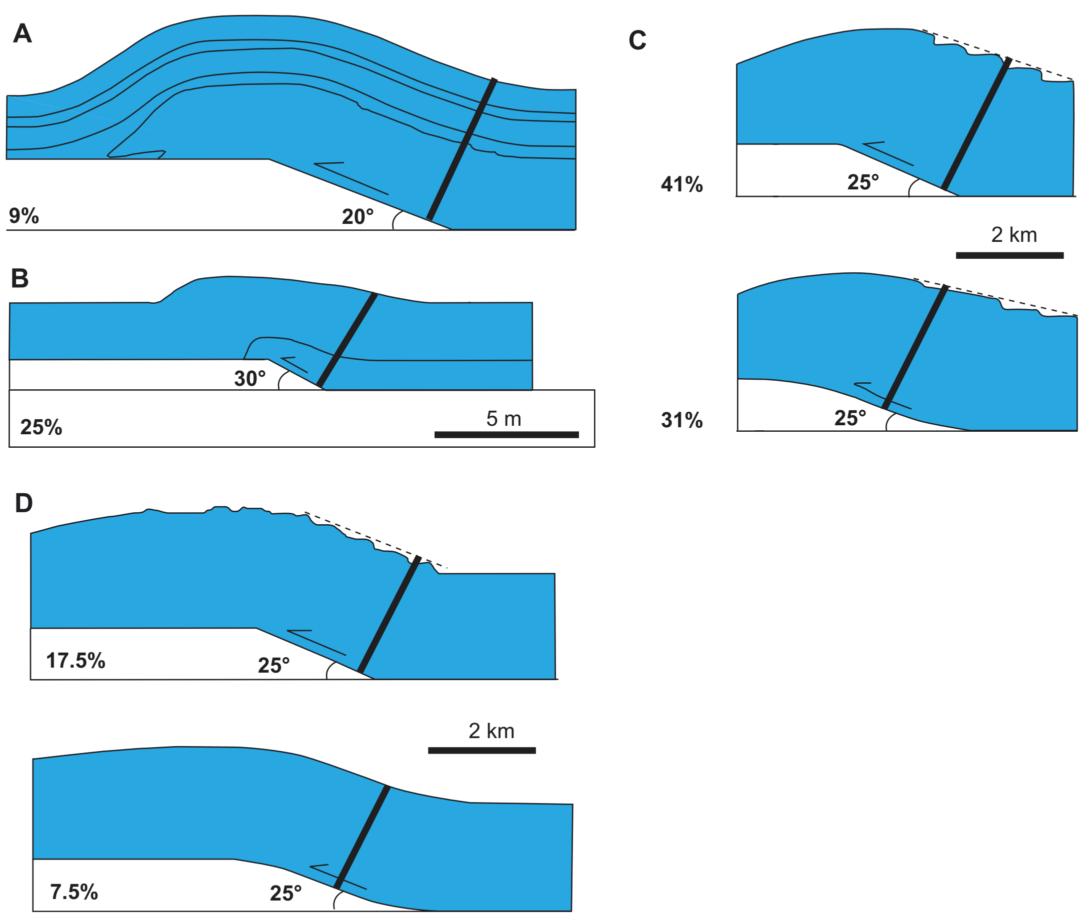

Fig. 5. Modified line drawings of (A) laboratory fault-bend fold by Chester et al. (1991), and numerical models by (B) Strayer and Hudleston (1997) and (C, D) Erickson et al. (2001), showing thickening of hanging-wall units during their transport over a ramp. Friction along the ramp in B is 0.1, in C is 0, and in D is 0.36. Undeformed thickness was measured above the flat and deformed thickness was measured perpendicular to the ramp (thick black lines).

sharp-bend ramp is two and one-half times (17.5%) the thickening (7%) above the frictionless round-bend ramp (Fig. 5D). Increasing the ramp friction ($\mu = 0.36$), increases the thickening to 41% and 31% over a sharp- and round-bend ramp, respectively, but preserves the effect of greater thickening at sharper ramps (Fig. 5C).

Measurements of the Erickson and Jamison (1995) finite-element models, where different mechanical properties were used, show that hanging-wall units thicken by 7.5% in uniform viscous models, 12% in uniform viscous-elastic models, and 27.5% in uniform plastic models when both hanging-wall and footwall units were deformable. However, in a viscous-plastic model, the hanging-wall units thickened by 22.5% when the footwall was rigid compared to 12% when the footwall was deformable.

6. Discussion and concluding remarks

Thickening of hanging-wall units above a ramp is clearly shown in laboratory experiments using sand, limestone and mica, as well as in numerical experiments for plastic, or viscous rheologies. It can also be predicted theoretically on the basis of minimum dissipation (Maillot and Leroy, 2003; Maillot and Koyi, 2006). Neglecting any diffuse deformation outside a single frictional back thrust and any dilatancy/compaction inside it, the theory predicts even greater thickening. The observation in analogue and numerical experiments, of more than half of the theoretical thickening, suggests that thickening is a robust feature of frictional (sand), cohesive (metal), or viscous ramp hanging-walls. In this respect, ramp friction and ramp dip both strongly promote thickening.

The examples presented here follow the usual geologic kinematics whereby the ramp is fixed with respect to the lower flat thrust above which the upper plate slides towards the ramp. In our box, as in many other studies, it is the ramp that is sliding on the basal plate. This experimental configuration guarantees that the thrusting of the sand occurs on the ramp surface. Alternatively, the sand layer can be pushed slowly above a viscous basal layer (e.g. Merle and Abidi, 1995), but smearing along the ramp precludes the steady-state that we were seeking in our experiments. We believe that these different basal shear conditions modify only marginally the amount of thickening in the ramp hanging wall, as suggested by the comparison of experiments RE6 and RE18 of Merle and Abidi (1995). Using a minimum dissipation criterion Maillot and Leroy (2003) showed theoretically that basal friction influences the thickening very little.

Our own models were restricted to the study of emerging ramps without relief build up, in contrast with most of the other studies discussed here. This simplification allowed us to study the hanging-wall thickening in the simplest conditions possible, as a steady-state process, independent of the total amount of bulk shortening, and thus to focus on effects of ramp dip and friction (Fig. 3A,B). The comparison with other models without erosion shows that the relief build-up modifies the absolute value of thickening but does not modify its dependency on the dip and friction values (Fig. 3).

The natural examples also show thickening (6.5% to 15%), but less than the laboratory and numerical experiments. Still, kinematic models that assume no hanging-wall thickening are used to interpret deformation along natural flat-ramp trajectories. Hence, a couple of clear questions emerge here: Do kinematic models correctly predict hanging-wall thickening in natural cases? Do hanging-wall units in natural cases thicken at all? If yes, why do then natural examples exhibit less thickening than in analogue and numerical experiments? Before discussing these questions, it is important to state that only models with relatively large ramp friction (0.7) and high ramp angle (45°), developed large amounts of hanging-wall thickening (80%). Obviously, friction along natural ramps at the time of deformation is not easy to determine, especially, when different lithologies are involved. However, our model results suggest that the small amount of thickening measured in the natural cases (6.5% to 15%) indicate a small magnitude of ramp friction along the gently dipping ramps. The relatively low figures of thickening measured from the natural cases could also be attributed to the rheology of the footwall units and their deformability. Unlike in the current models where the footwall is rigid (i.e. undeformable), in natural examples, the footwall is likely to deform and reduce the total strain in the hanging-wall units. This is supported by the results of Erickson et al. (2001), where in models with non-deformable footwall, hanging-wall units thicken almost twice (22.5%) as much as in models with deformable footwall (12%). In addition, in the Stellarton (Nova Scotia) example (Waldron, 2004), footwall and hanging-wall thickening individually (14% and 7%, respectively) was less than the total thickening (21%). In this example, the hanging-wall is thickened much less than the deformable footwall.

The deformation mechanism in models is unlikely to mimic that of the natural cases in all aspects. During deformation of the sand layer over the ramp, repacking of the sand grains results in a bulk volume loss, while dilatancy increases volume along the thrusts. However, it should be clear that hanging-wall thickening is not due to this, but is merely a consequence of the fact that the thrusts forming from the base of the ramp to the surface have a dip less than the bisecting angle between the lower flat and the ramp. Should the thrusts bisect the angle between lower flat and ramp, as assumed in the fault-bend fold kinematic model for example, there would be no thickening. The same holds for the natural examples (and the numerical ones), although more complex deformations mechanisms alter this simple picture, depending on the scale and conditions of each example: diffuse volumetric deformation, layer parallel shortening/compaction, folding, etc. In the particular case of flexural slip, the back thrust is replaced by a hinge zone where layers rotate continuously to become parallel to the ramp. Although these natural deformation mechanisms differ radically from those of the sand, the overall tectonic thickening is still controlled by the dip of the hinge in the same way as back thrusts in sand. Maillot and Leroy (2003) showed theoretically that a ductile hinge with flexural slip also leads to thickening because its optimal dip with respect to dissipation does not bisect the angle between lower flat and ramp.

We finally discuss how a theoretical approach could be developed to account for all these observations of thickening. The commonly used constant-thickness kinematic models do not account for hanging-wall thickening. The question of knowing when to amend a kinematic model to account for this thickening is not an easy one. In the light of the present study, it is clear that a prediction of hanging-wall thickening will necessarily make use of mechanical concepts such as force balance and rheology, and cannot be restricted only to geometrical considerations. In an earlier work (Maillot and Leroy, 2003), we used global force balance and the principle of minimum dissipation to show analytically that the classic fault-bend fold kinematic model leads to an important excess of energy dissipation with respect to an amended kinematic model accounting for hanging-wall thickening. This result was demonstrated for both brittle and ductile materials (with flexural slip) and in simple steady-state conditions, i.e. without relief build up. These predictions were then validated experimentally with sand box models by Maillot and Koyi (2006), again with full erosion of any topographic relief. Although our new experiments are also in steady-state conditions, we acknowledge the importance of the evolution of structures due to the relief build up, as shown by the numerous examples presented here, whether analogue, numerical, or natural. However, it is also clear that relief build up is not a necessary, nor a sufficient condition for thickening. It certainly modifies its magnitude but does not trigger or preclude it. Our previous theoretical work can be improved in two ways: first, the principle of minimum dissipation (which is not a law of physics) can be replaced by the maximum strength theorem well known in soil mechanics (Salençon, 1974), and second, the evolution of a structure can be described by applying this theorem at every step. These techniques have been applied to the onset and growth of a kink fold (Maillot and Leroy, 2006) and should give a useful theoretical framework to study the transitory response due to relief build up, or also strain softening, and therefore should help in predicting better hanging-wall thickening.

In conclusion, hanging-wall units can thicken when passing from a lower flat to a ramp, unlike in the kinematic models typically used to describe structural geometries above footwall ramps. Analysis of our models, of other published analogue and numerical models, and of our theoretical predictions show that this thickening is largely controlled by the ramp dip, friction, and shape. In nature, this thickening may be manifested in folding, imbrication and penetrative strain, which results in a bulk tectonic thickening of the hanging-wall units during their transport from the flat to the ramp.

Acknowledgments

Thanks are due to Dominique Frizon and Paul-Emille Guezou for comments, Heng Fa and John Waldron for giving permission to publish their field photographs in Fig. 4. We also thank B. A. Couzens-Schultz for a thorough and constructive review, Peter Cobbold and an anonymous reviewer for comments, and finally the editor, Dr. William Dunne, for a thorough and professional review and editing of this article. H.A.K. is funded by the Swedish Research Council (VR). B.M. is funded by a research agreement with the Institut Français du Pétrole, and benefited from a teaching sabbatical leave financed by the CNRS and the scientific council of the University of Cergy-Pontoise.

References

Apperson, K.D., Goff, D.F., 1991. Deformation of thrust ramps and footwalls observed in numerical models. EOS (Transactions, American Geophysical Union) 72, 514–515.

Bahroudi, A., Koyi, H.A., 2003. The effect of spatial distribution of Hormuz salt on deformation style in the Zagros fold and thrust belt: an analogue modeling approach. Journal of the Geological Society (London) 160, 719–733.

Berger, P., Johnson, A.M., 1980. First-order analysis of deformation of a thrust sheet moving over a ramp. Tectonophysics 70, T9–T24.

Bonini, M., 2001. Passive roof thrusting and foreland-ward fold propagation in scaled brittle-ductile physical models of thrust wedges. Journal of Geophysical Research 106, 2291–2311.

Cristallini, E.O., Allmendinger, R.W., 2002. Backlimb trishear: a kinematic model for curved folds developed over angular fault bends. Journal of Structural Geology 24, 289–295.

Chester, J., Chester, F., 1990. Fault propagation folds above thrusts with constant dip. Journal of Structural Geology 12, 903–910.

Chester, J.S., Logan, J.M., Spang, J.H., 1991. Influence of layering and boundary conditions on fault-bend and fault-propagation folding. Geological Society of America Bulletin 103, 1059–1072.

Cook, D.G., MacLean, B.C., 1999. The Imperial anticline, a fault-bend fold above a bedding-parallel thrust ramp, Northwest Territories, Canada. Journal of Structural Geology 21, 215–228.

Cotton, J.T., Koyi, H.A., 2000. Modeling of thrust fronts above ductile and frictional decollements: application to structures in the salt range and potwar plateau, Pakistan. Geological Society of America Bulletin 112, 351–363.

Davis, D.M., Engelder, T., 1985. The role of salt in fold-and-thrust belts. Tectonophysics 119, 67–88.

Dahlstrom, C.D.A., 1969. The upper detachment in concentric folding. Bulletin of Canadian Petroleum Geology 17, 326–346.

Dahlstrom, C.D.A., 1990. Geometric constraints derived from the law of conservation of volume and applied to evolutionary models for detachment folding. American Association of Petroleum Geologists Bulletin 74, 336–344.

Di Toro, G., Goldsby, D.L., Tullis, T.E., 2004. Friction falls towards zero in quartz rock as slip velocity approaches seismic rates. Nature 427, 436–439.

Erickson, S.G., Jamison, W.R., 1995. Viscous-plastic finite-element models of fault-bend folds. Journal of Structural Geology 17, 561–573.

Erickson, S.G., Strayer, L.M., Suppe, J., 2001. Initiation and reactivation of faults during movement over a thrust-fault ramp: Numerical mechanical models. Journal of Structural Geology 23, 11–23.

Fischer, M.P., Woodward, N.B., Mitchell, M.M., 1992. The kinematics of break-thrust folds. Journal of Structural Geology 14, 451–460.

Jamison, W.R., 1987. Geometric analysis of fold development in overthrust terranes. Journal of Structural Geology 9, 207–219.

Kattenhorn, S.A., 1994. Outcrop-scale fault-related folds, Valley and Ridge province, Appalachians: comparison to kinematic model predictions: M.S. thesis, University of Akron, Ohio, 124 pp.

Kilsdonk, B., Fletcher, R.C., 1989. An analytical model of hanging-wall and footwall deformation at ramps on normal and thrust faults. Tectonophysics 163, 153–168.

Koyi, H.A., 1995. Mode of internal deformation in model accretionary wedges. Journal of Structural Geology 17 (2), 293–300.

Koyi, H.A., Vendeville, B., 2004. The effect of décollement dip on geometry and kinematics of model accretionary wedges. Journal of Structural Geology 25 (9), 1445–1450.

Koyi, H.A., Sans, M., Teixell, A., Cotton, J., Zeyen, H., 2004. The significance of penetrative strain in the restoration of shortened layers—Insights from sand models and the Spanish Pyrenees. In: McClay, K.R. (Ed.), Thrust Tectonics and Petroleum Systems. American Association of Petroleum Geologists Memoir 82, pp. 207–222.

Koyi, H.A., Cotton, J., 2004. Experimental insights on the geometry and kinematics of fold-and-thrust belts above weak, viscous evaporitic decollement; a discussion. Journal of Structural Geology 26, 2139–2141.

Letouzey, J., Colletta, B., Vially, R., Chermette, J.C., 1995. Evolution of salt-related structures in compressional settings. In: Jackson, M.P.A., Roberts, D.G., Snelson, S. (Eds.), Salt Tectonics. A global Perspective. American Association of Petroleum Geologists Memoir 65, pp. 41–60.

Maillot, B., Koyi, H.A., 2006. Thrust dips and thrust refraction in fault-bend faults: analogue experiments and theoretical predictions. Journal of Structural Geology 28, 36–49.

Maillot, B., Leroy, Y.M., 2003. Optimal dip based on dissipation of back thrusts and hinges in fold-and-thrust belts. Journal of Geophysical Research 108, (B6), 2320–2336.

Maillot, B., Leroy, Y.M., 2006. Kink-fold onset and development based on the maximum strength theorem. Journal of the Mechanics and Physics of Solids 54, 2030–2059.

Maillot, B., Barnes, C., Mengus, J.-M., Daniel, J.-M., 2007. Constraints on friction coefficients by an inverse analysis of sand box thrust dips. Journal of Structural Geology 29, 117–128.

Marone, C., Saffer, D.M., Frye, K.M., 1999. Weak and potentially unstable frictional behavior of smectite clay. EOS(Transactions, American Geophysical Union) 80 (46), F689.

McNaught, M.A., Mitra, G., 1993. A kinematic model for the origin of footwall synclines. Journal of Structural Geology 15, 805–808.

Mercier, E., Outtani, F., Frizon de Lamotte, D., 1997. Late stage evolution of fault-propagation fold: principles and examples. Journal of Structural Geology 19, 185–193.

Merle, O., Abidi, N., 1995. Approche expérimentale du fonctionnement des rampes émergentes. Bulletin de la Société Géologique de France 166 (5), 439–450.

Mitra, S., 1990. Fault-propagation folds: Geometry, kinematic evolution, and hydrocarbon traps. American Association of Petroleum Geologists Bulletin 74, 921–945.

Mitra, S., 1992. Balanced structural interpretations in fold and thrust belts. In: Mitra, S., Fisher, G.W. (Eds.), Structural Geology of Fold and Thrust Belts. Johns Hopkins University Press, Baltimore, pp. 53–77.

Persson, K., 2001. Effective indenters and the development of double-vergent orogens; insights from analogue sand models. In: Koyi, H.A., Mancktelow, N.S. (Eds.), Tectonic Modeling; A Volume in Honor of Hans Ramberg. Geological Society of America Memoir 193, pp. 191–206.

Poblet, J., McClay, K., 1996. Geometry and kinematics of single-layer detachment folds. American Association of Petroleum Geologists Bulletin 80, 1085–1109.

Ramsay, J.G., 1992. Some geometric problems of ramp-flat thrust models. In: McClay, K.R. (Ed.), Thrust Tectonics. Chapman & Hall, London, pp. 191–200.

Rich, J.L., 1934. Mechanics of low-angle overthrust faulting as illustrated by Cumberland thrust block, Virginia, Kentucky and Tennessee. American Association of Petroleum Geologists Bulletin 33, 1643–1654.

Salençon, J., 1974. Théorie de la plasticité pour les applications à la mécanique des sols. Editions Eyrolles, Paris. English translation: Applications of the Theory of Plasticity in Soil Mechanics. Wiley, New York, 1977.

Smart, K.J., Couzens-Schultz, B.A., 2001. Mechanics of blind thrusting: Comparison of numerical and physical modeling. The Journal of Geology 109, 771–779.

Strayer, L.M., Hudleston, P.J., 1997. Numerical modeling of fold initiation at thrust ramps. Journal of Structural Geology 19, 551–566.

Suppe, J., 1983. Geometry and kinematics of fault-bend folding. American Journal of Science 283, 684–721.

Suppe, J., 1985. Principles of Structural Geology. Prentice-Hall, Englewood Cliffs, NJ, 537 pp.

Suppe, J., Medwedeff, D.A., 1990. Geometry and kinematics of fault-propagation folding. Eclogae Geologicae Helvetiae 83, 409–454.

Waldron, J.W.F., 2004. Anatomy and evolution of a pull-apart basin, Stellarton, Nova Scotia. Geological Society of America Bulletin 116, 109–127.

Wickham, 1995. Fault displacement-gradient folds and the structure at Lost Hills, California (USA). Journal of Structural Geology 17, 1293–1302.

Willis, B., Willis, R., 1934. Geologic structures. McGraw Hill, New York, 544 pp.

Wiltschko, D.V., 1979. A mechanical model for thrust sheet deformation at a ramp. Journal of Geophysical Research 84, 1091–1104.

Withjack, M.O., Peterson, E.T., 1993. Prediction of normal-fault geometries—a sensitivity analysis. American Association of Petroleum Geologists Bulletin 77 (11), 1860–1873.